

# Do Finite Density Effects Jeopardize Axion Nucleophobia in Supernovae?

Luca Di Luzio,<sup>1,\*</sup> Vincenzo Fiorentino,<sup>2,3,4,†</sup>  
Maurizio Giannotti,<sup>5,6,‡</sup> Federico Mescia,<sup>3,7,§</sup> and Enrico Nardi<sup>3,8,¶</sup>

<sup>1</sup>*Istituto Nazionale di Fisica Nucleare, Sezione di Padova, Via F. Marzolo 8, 35131 Padova, Italy*

<sup>2</sup>*Dipartimento di Fisica e Astronomia ‘G. Galilei’,  
Università di Padova, Via F. Marzolo 8, 35131 Padova, Italy*

<sup>3</sup>*Istituto Nazionale di Fisica Nucleare, Laboratori Nazionali di Frascati, 00044 Frascati, Italy*

<sup>4</sup>*Università degli Studi Roma Tre, Via della Vasca Navale 84, I-00146, Rome, Italy*

<sup>5</sup>*Centro de Astropartículas y Física de Altas Energías,  
University of Zaragoza, Zaragoza, 50009, Aragón, Spain*

<sup>6</sup>*Department of Chemistry and Physics, Barry University,  
Miami Shores, 33161, FL, United States of America*

<sup>7</sup>*On leave of absence from Universitat de Barcelona*

<sup>8</sup>*Laboratory of High Energy and Computational Physics,  
HEPC-NICPB, Rävåla 10, 10143 Tallinn, Estonia*

Nucleophobic axion models, wherein axion couplings to both protons and neutrons are simultaneously suppressed, can relax the stringent constraints from SN 1987A. However, it remains uncertain whether these models maintain their nucleophobic property under the influence of finite baryon density effects. These are especially relevant in astrophysical environments near saturation density, such as Supernovae (SNe). In this study, we demonstrate that the nucleophobic solution remains viable also at finite density. Furthermore, we show that the SN axion bound relaxes significantly in nucleophobic models, even when accounting for the integration over the non-homogeneous environment of the SN core.

## I. INTRODUCTION

The Quantum Chromodynamics (QCD) axion offers a compelling solution to the strong CP problem [1–4] and serves as an excellent dark matter candidate [5–7], thereby addressing two major challenges in contemporary high-energy physics. The axion’s model-independent properties are primarily determined by a single parameter, the axion decay constant,  $f_a$ , which determines the value of the axion mass,  $m_a$ , and the overall suppression of the axion couplings to Standard Model (SM) particles. The actual strength of a specific coupling, however, crucially depends also on the particular axion model under consideration, through the Wilson coefficients of the axion effective Lagrangian (see e.g. [8]). This fact is especially important when addressing astrophysical constraints on the axion parameter space, which are often presented in terms of benchmark KSVZ [9, 10] and DFSZ [11, 12] axion models.

In Ref. [13], a new class of axion models, termed “astrophobic”, was shown to simultaneously suppress the axion’s couplings to nucleons and electrons, thereby loosening the stringent bounds imposed by Supernova (SN) 1987A [14, 15], as well as by the observed evolution of red giants [16, 17] and white dwarfs [18, 19]. In this case, the astrophysical constraints on the axion mass can be relaxed by more than one order of magnitude, compared to, for example, the benchmark KSVZ model.

It should be noted that achieving the nucleopho-

bic condition in a QCD axion context is non-trivial, due to the irreducible contribution to the axion-nucleon coupling arising from the anomalous axion-gluon interaction. In fact, it can be seen that in benchmark axion models it is not possible to simultaneously suppress the axion coupling to both protons and neutrons. Remarkably, the nucleophobic conditions necessarily require a non-universal Peccei-Quinn (PQ) charge assignment [13], where SM quarks from different generations carry distinct PQ charges, thus establishing an intriguing link with flavour physics.

The nucleophobic conditions were originally established at tree level [13]. However, since they rely on a mild  $\mathcal{O}(10\%)$  tuning, it was essential to ascertain that renormalization group (RG) effects do not undermine the whole construction. This was verified in Ref. [20], where it was shown that RG running simply shifts the parameter space region where the nucleophobic conditions are realised.

In this work, we address another issue concerning the stability of the nucleophobic conditions against a different class of corrections. The SN 1987A bound arises from constraints on axion emission from a highly dense stellar environment, where axion interactions with nucleons are significantly affected by in-medium corrections, as recently demonstrated in Ref. [21] (see also [22, 23]). In particular, since the baryonic density  $n/n_0$  (normalized to the nuclear saturation density  $n_0 \simeq 0.16 \text{ fm}^{-3}$ ) varies significantly along the SN radius (cf. Fig. 1), even if nucleophobia can be enforced locally for a given  $n/n_0$ , it is unclear whether the axion emissivity integrated over the SN core would still exhibit a suppression comparable to the one observed with axion couplings in vacuum. The purpose of this work is to quantitatively assess to which extent nucleophobic axion

\* [luca.diluzio@pd.infn.it](mailto:luca.diluzio@pd.infn.it)

† [vincenzo.fiorentino@uniroma3.it](mailto:vincenzo.fiorentino@uniroma3.it)

‡ [mgiannotti@unizar.es](mailto:mgiannotti@unizar.es)

§ [federico.mescia@lnf.infn.it](mailto:federico.mescia@lnf.infn.it)

¶ [enrico.nardi@lnf.infn.it](mailto:enrico.nardi@lnf.infn.it)

models can be regarded as realistic possibilities that endure finite density effects in SNe.

The outline of this paper is as follows. In Sec. II, we review nucleophobic axions in vacuum. Sec. III provides an overview of finite density effects in SNe, followed in Sec. IV by an analysis of finite density corrections to axion-nucleon couplings and by an assessment of the fate of nucleophobic axion models under realistic finite density conditions in Sec. V. Finally, in Sec. VI we present our conclusions.

## II. NUCLEOPHOBIC AXIONS IN VACUUM

Before discussing finite density effects, we begin by introducing axion-nucleon couplings in vacuum, we review the structure of nucleophobic axion models and outline the nucleophobic conditions.

### A. Axion-nucleon couplings in vacuum

The axion couplings to nucleons,  $N = p, n$ , defined via the Lagrangian term

$$c_N \frac{\partial_\mu a}{2f_a} \bar{N} \gamma^\mu \gamma_5 N, \quad (1)$$

can be computed in the framework of Heavy Baryon Chiral Perturbation Theory (HBChPT), a non-relativistic effective field theory where nucleons are at rest and the axion is treated as an external current (see [24–26] for details). In particular, working at leading order with three active flavours, one obtains

$$c_p = \left( c_u - \frac{1}{1+z+w} \right) \Delta_u + \left( c_d - \frac{z}{1+z+w} \right) \Delta_d + \left( c_s - \frac{w}{1+z+w} \right) \Delta_s, \quad (2)$$

$$c_n = \left( c_u - \frac{1}{1+z+w} \right) \Delta_d + \left( c_d - \frac{z}{1+z+w} \right) \Delta_u + \left( c_s - \frac{w}{1+z+w} \right) \Delta_s, \quad (3)$$

where  $c_{u,d,s} \equiv c_{u,d,s}(2 \text{ GeV})$  are low-energy axion couplings to quarks, defined analogously to Eq. (1), and evaluated at the scale  $\mu = 2 \text{ GeV}$  by numerically solving the RG equations [27–30] from the boundary values  $c_{u,d,s}(f_a)$  (see below). For the quark mass ratios we have  $z = m_u(2 \text{ GeV})/m_d(2 \text{ GeV}) = 0.465(24)$  [31, 32], and  $w = m_u(2 \text{ GeV})/m_s(2 \text{ GeV}) = 0.0233(9)$  [33–36].  $\Delta_q$ , with  $q = u, d, s$ , are hadronic matrix elements encoding the contribution of a quark  $q$  to the spin operator  $S^\mu$  of the proton, defined via  $S^\mu \Delta q = \langle p | \bar{q} \gamma^\mu \gamma_5 q | p \rangle$ . In particular,  $g_A = \Delta_u - \Delta_d = 1.2754(13)$  is extracted from  $\beta$ -decays [37], while  $\Delta_u = 0.847(18)(32)$ ,  $\Delta_d = -0.407(16)(18)$  and  $\Delta_s = -0.035(6)(7)$  (at 2 GeV in the  $\overline{\text{MS}}$  scheme) are the  $N_f = 2 + 1$  FLAG 2024 averages [38, 39],

dominated by the results in Ref. [40]. For further reference, we also define the iso-singlet combination  $g_0^{ud} = \Delta_u + \Delta_d = 0.44(4)$ .

Running effects on the low-energy axion couplings to light quarks can be parametrized as [41]

$$c_{u,d,s} \simeq c_{u,d,s}^0 + r_{u,d,s}^t c_t^0, \quad (4)$$

where  $c_{u,d,s,t}^0 \equiv c_{u,d,s,t}(f_a)$  are axion couplings defined at the UV scale  $\mu = f_a$ , the parameters  $r_{u,d,s}^t$  encode the RG correction approximated by taking the leading one-loop top-Yukawa contribution, and depend logarithmically on the mass scale of the heavy scalar degrees of freedom in the UV completion of the axion model, which is assumed to be of  $\mathcal{O}(f_a)$ . The values of  $r_{u,d,s}^t$ , obtained by interpolating the numerical solution to the RG equations, are tabulated in Appendix B of Ref. [30]. In the following, we will set as a reference value,  $f_a = 10^8 \text{ GeV}$ , corresponding to  $r_u^t = -0.2276$  and  $r_{d,s}^t = 0.2290$ , and we neglect the small logarithmic dependence from shifts in  $f_a$  when varying the axion mass.

### B. Nucleophobic conditions in vacuum

In order to discuss nucleophobic axion models, in which the axion couplings to protons and neutrons are simultaneously suppressed, it is convenient to consider the combinations

$$c_p + c_n = \left( c_u + c_d - \frac{1+z}{1+z+w} \right) g_0^{ud} + 2 \left( c_s - \frac{w}{1+z+w} \right) \Delta_s \simeq (c_u^0 + c_d^0 - 1) g_0^{ud} + 2(c_s^0 + r_s^t c_t^0) \Delta_s, \quad (5)$$

$$c_p - c_n = \left( c_u - c_d - \frac{1-z}{1+z+w} \right) g_A \simeq \left( c_u^0 - c_d^0 + (r_u^t - r_d^t) c_t^0 - \frac{1-z}{1+z} \right) g_A, \quad (6)$$

where in the last step we neglected  $\mathcal{O}(w)$  corrections and we have employed the approximation  $r_u^t + r_d^t \simeq 0$  (both approximations hold at the per mil level). Neglecting also  $2c_s \Delta_s$  in Eq. (5), that amounts to a few percent (the precise value depending on the specific axion model), we see that nucleophobia requires the following condition between UV axion couplings

$$c_u^0 + c_d^0 = 1. \quad (7)$$

This condition can be enforced exactly in terms of non-universal PQ charges, and implies  $c_p + c_n \simeq 0$ . In contrast, to ensure that  $c_p - c_n \simeq 0$  as well, requires tuning  $c_u^0 - c_d^0$  against the remainder terms in Eq. (6):

$$c_u^0 - c_d^0 = \frac{1-z}{1+z} - (r_u^t - r_d^t) c_t^0, \quad (8)$$

which provides the second nucleophobic condition. Note that the residual contribution to the axion-nucleon couplings is eventually set by the  $2c_s \Delta_s$  term in the last line of Eq. (5).

### C. Nucleophobic axion models

Different realization of nucleophobic axion models were proposed in Ref. [13] (see also [42–49] for model-building variants). Here, we consider for definiteness the model denoted as M1 in Ref. [13], although our conclusions apply more generally also to other nucleophobic axion models.

The M1 model features the same scalar sector of the standard DFSZ model [11, 12], namely a complex scalar, singlet under  $SU(3)_c \times SU(2)_L \times U(1)_Y$ ,  $\Phi \sim (1, 1, 0)$  and two Higgs doublets  $H_{1,2} \sim (1, 2, -1/2)$ , which are coupled in the scalar potential via the non-hermitian operator  $H_2^\dagger H_1 \Phi$ . The vacuum angle is defined by  $\tan \beta = \langle H_2 \rangle / \langle H_1 \rangle$ , so that the requirement that the PQ current is orthogonal to the hypercharge current fixes the PQ charges of the two Higgs doublets as  $\mathcal{X}_1 = -\sin_\beta^2 \equiv -s_\beta^2$  and  $\mathcal{X}_2 = \cos_\beta^2 \equiv c_\beta^2$ , while  $\mathcal{X}_\Phi = 1$  by normalization. The M1 model is further characterized by a 2+1 structure of the PQ charge assignments, namely two generations replicate the same set of PQ charges. Note that, as explained in Ref. [13], in this case all the entries in the up- and down-type quark Yukawa matrices are allowed and there are no texture zeros. In particular, the Yukawa sector of the M1 model contains the following operators

$$\begin{aligned} & \bar{q}_\alpha u_\beta H_1, \quad \bar{q}_3 u_3 H_2, \quad \bar{q}_\alpha u_3 H_1, \quad \bar{q}_3 u_\beta H_2, \\ & \bar{q}_\alpha d_\beta \tilde{H}_2, \quad \bar{q}_3 d_3 \tilde{H}_1, \quad \bar{q}_\alpha d_3 \tilde{H}_2, \quad \bar{q}_3 d_\beta \tilde{H}_1, \\ & \bar{\ell}_\alpha e_\beta \tilde{H}_1, \quad \bar{\ell}_3 e_3 \tilde{H}_2, \quad \bar{\ell}_\alpha e_3 \tilde{H}_1, \quad \bar{\ell}_3 e_\beta \tilde{H}_2, \end{aligned} \quad (9)$$

where  $\alpha, \beta = 1, 2$  span over first and second generations, while  $q, \ell$  denote left-handed (LH) doublets and  $u, d, e$  right-handed (RH) singlets. The PQ charges stemming from the Yukawa sector in Eq. (9) read

$$\begin{aligned} \mathcal{X}_{q_i} &= (0, 0, 1), \\ \mathcal{X}_{u_i} &= (s_\beta^2, s_\beta^2, s_\beta^2), \\ \mathcal{X}_{d_i} &= (c_\beta^2, c_\beta^2, c_\beta^2), \\ \mathcal{X}_{\ell_i} &= -\mathcal{X}_{q_i}, \quad \mathcal{X}_{e_i} = -\mathcal{X}_{u_i}. \end{aligned} \quad (10)$$

The associated anomaly coefficients are  $E/N = 2/3$  and  $2N = 1$  (cf. [8] for standard notation), while the mixing-independent part of the axion couplings to SM fermions are

$$\begin{aligned} c_{u,c}^0 &= s_\beta^2, & c_t^0 &= -c_\beta^2, \\ c_{d,s}^0 &= c_\beta^2, & c_b^0 &= -s_\beta^2, \\ c_{e,\mu}^0 &= -s_\beta^2, & c_\tau^0 &= c_\beta^2, \end{aligned} \quad (11)$$

with  $\tan \beta \in [0.25, 170]$  set by perturbativity [42]. Since the charges of the RH fields are generation independent, there are no corrections from RH mixings. In the LH sector mixing effects can play a role because the third generation has different charges from the first two. For the quarks, we assume that the LH mixing matrix has CKM-like entries, so that mixing effects are small and will be neglected.

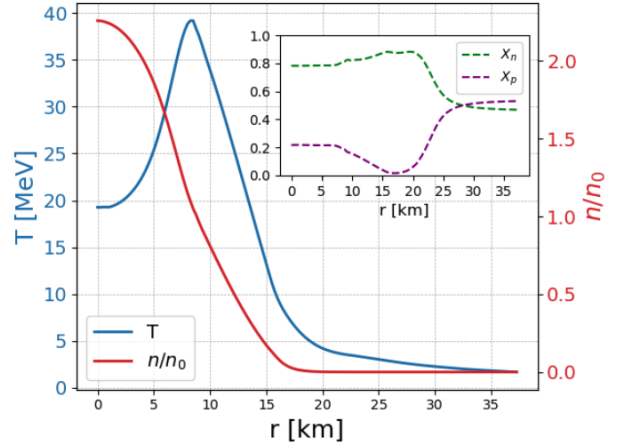


FIG. 1. Temperature and density profiles of the SN model from Ref. [50], used in this work, as a function of the distance from the center of the star  $r$ , 1 s after bounce. The inset shows the neutron ( $X_n$ ) and proton ( $X_p$ ) fractions, again as a function of  $r$  in km. See text for more details.

From Eq. (11) it follows that the first nucleophobic condition in Eq. (7) is automatically satisfied, while  $c_u^0 - c_d^0 = s_\beta^2 - c_\beta^2$ . Neglecting RG effects, the second nucleophobic condition in Eq. (8) is approximately satisfied for  $\tan \beta \simeq \sqrt{2}$ . On the other hand, as argued in Ref. [20], RG effects are relevant for the second nucleophobic condition and their role is that of changing the cancellation point, that in the M1 model gets shifted to  $\tan \beta \simeq 1.19$ . Hence, although the shift in the parameter space region where the nucleophobic condition is realised is sizeable, running effects do not prevent the possibility of having nucleophobic models.

The calculation of the axion-nucleon coupling has been done so far assuming zero density. However, since the primary relevance of considering nucleophobic axion models lies in their application to the astrophysical environment of SNe, it is mandatory to ask whether the nucleophobic conditions can still be realised once finite density effects are taken into account. In the following, in order to assess the fate of nucleophobic axion models at finite density, we first provide an overview of density effects in SNe, and then we discuss finite density corrections to axion-nucleon couplings.

### III. OVERVIEW OF DENSITY EFFECTS IN SUPERNOVAE

SN cores are extremely dense object, whose baryonic number density,  $n = n_p + n_n$ , is of the order of the nuclear saturation density  $n_0 \simeq 0.16 \text{ fm}^{-3}$ , i.e. the baryon number density found in nuclei. The density and temperature profiles of a realistic SN model, 1 s after bounce, are shown in Fig. 1, including the neutron ( $X_n = n_n/n$ ) and proton ( $X_p = n_p/n$ ) fractions. The model refers to the GARCHING group’s SN model SFHo-s18.8, pro-

vided in Ref. [50], based on the PROMETHEUS-VERTEX [51] code, with the SFHo Equation of State (EoS) [52, 53]. The model considers a  $18.8M_\odot$  stellar progenitor [54] and predicts a neutron star with baryonic mass  $1.35M_\odot$ .

The production of axions inside a SN can be influenced in a non-negligible way by the dense nuclear medium. Hence, in order to obtain a reliable bound from the cooling argument, it is necessary to determine how finite density corrections affect axion-nucleon interactions, that determine the rate of axion emission from SNe.

Certain finite density effects that are quite important in the calculation of the axion emission rate have already been identified in previous studies (see, e.g., [14, 15, 55]). For example, if nucleons are sufficiently close to each other, as is the case for densities near  $n_0$ , the repulsive nuclear forces cannot be neglected and these induce changes in the nucleons dispersion relations

$$E_N \simeq m_N + \frac{|p_N|^2}{2m_N^*} + U_N, \quad (12)$$

where  $U_N = \Sigma_N^S + \Sigma_N^V$  is the non-relativistic mean-field potential containing contributions of the scalar ( $\Sigma_N^S$ ) and vector ( $\Sigma_N^V$ ) self-energies (see e.g. [56]). The scalar contribution,  $\Sigma_N^S$ , provides the well-known correction to the nucleon mass  $m_N^* = m_N + \Sigma_N^S$ . These effects can be quite significant in the core of a SN, and, for example, can reduce the neutron mass by about a factor of two. However, these calculations have not taken into account the modifications to the axion-nucleon couplings that are introduced when the interactions occur inside a highly dense medium.

#### IV. NUCLEOPHOBIC AXIONS AT FINITE DENSITY

We proceed now to assess the impact of finite density corrections on nucleophobic axion models. First, we review the main formalism developed in Ref. [21] for in-medium corrections to axion-nucleon couplings and then discuss their impact on axion nucleophobia.

##### A. Axion-nucleon couplings at finite density

Finite density corrections to axion-nucleon couplings were recently computed in Ref. [21]. There are basically two independent effects to be taken into account: the modification of the axion potential due to the change of the chiral condensates and the in-medium corrections to the axial couplings  $g_A$  (iso-triplet) and  $g_{ud}^0$  (iso-singlet).

The change in the chiral condensates at finite density can be parametrized using the Hellmann-

Feynman theorem [57]

$$\zeta_{\bar{q}q}(n) \equiv \frac{\langle \bar{q}q \rangle_n}{\langle \bar{q}q \rangle_0} = 1 + \frac{1}{\langle \bar{q}q \rangle_0} \frac{\partial \Delta E(n)}{\partial m_q}, \quad (13)$$

with  $q = u, d, s$ , and the subscripts  $n$  and  $0$  denoting respectively the in-medium and in-vacuum values. Here,  $\Delta E(n)$  represents the shift in the QCD ground state energy due to the nucleonic background. Neglecting both nuclear interactions and relativistic corrections, one has the linear approximation for the chiral condensates,  $\Delta E = \sum_{N=n,p} m_N n_N$ . This allows to cast the shift in the condensates in terms of the partial derivatives  $\partial m_N / \partial m_q$ , which are directly related to the so-called sigma terms. In particular, one obtains [21]

$$\zeta_{\bar{u}u}(n) = 1 - b_1 \frac{n}{n_0} + b_2 \left[ 2 \frac{n_p}{n} - 1 \right] \frac{n}{n_0}, \quad (14)$$

$$\zeta_{\bar{d}d}(n) = 1 - b_1 \frac{n}{n_0} - b_2 \left[ 2 \frac{n_p}{n} - 1 \right] \frac{n}{n_0}, \quad (15)$$

$$\zeta_{\bar{s}s}(n) = 1 - b_3 \frac{n}{n_0}, \quad (16)$$

where  $n = n_p + n_n$  and we defined the  $b$ -coefficients

$$b_1 \equiv \frac{\sigma_{\pi N} n_0}{m_\pi^2 f_\pi^2} = 3.5 \times 10^{-1} \left( \frac{\sigma_{\pi N}}{45 \text{ MeV}} \right), \quad (17)$$

$$b_2 \equiv \frac{\tilde{\sigma}_{\pi N} n_0}{m_\pi^2 f_\pi^2} \frac{m_u + m_d}{m_u - m_d} = -2.2 \times 10^{-2} \left( \frac{\tilde{\sigma}_{\pi N}}{1 \text{ MeV}} \right),$$

$$b_3 \equiv \frac{\tilde{\sigma}_s n_0}{m_\pi^2 f_\pi^2} \frac{m_u + m_d}{m_s} = 1.7 \times 10^{-2} \left( \frac{\sigma_s}{30 \text{ MeV}} \right),$$

and the sigma terms (defined as in Ref. [21]) have been normalized to their central values [21, 58]. Note that the  $\langle \bar{s}s \rangle_n$  condensate is weakly affected by the nucleonic background, while  $\langle \bar{u}u \rangle_n \simeq \langle \bar{d}d \rangle_n$  up to a small isospin correction [59].

In the following, we will consider only the regime  $n < n_c \equiv n_0/b_1 \simeq 2.8 n_0$ , with  $n_c$  being the critical density in which one naively expects chiral symmetry restoration in the linear approximation. The validity of the linear approximation for the in-medium shift of the chiral condensates was estimated to be  $n/n_0 \lesssim 1 \div 2$  by including relativistic corrections to the energy of the nucleons [21] (see also [60, 61]).

The change in the chiral condensates at finite density can be tracked by correcting the quark masses as  $m_q \rightarrow (\langle \bar{q}q \rangle_n / \langle \bar{q}q \rangle_0) m_q$ . For the axion-nucleon couplings at finite density, this implies that one should replace in Eqs. (2)–(3)  $z \rightarrow zZ$  and  $w \rightarrow wW$ , with

$$Z \equiv \frac{\langle \bar{u}u \rangle_n}{\langle \bar{d}d \rangle_n} = 1 - 2b_2 \frac{n_n - n_p}{n_0}, \quad (18)$$

$$W \equiv \frac{\langle \bar{u}u \rangle_n}{\langle \bar{s}s \rangle_n} = 1 - \left[ b_1 + b_2 \left( 1 - \frac{2n_p}{n} \right) - b_3 \right] \frac{n}{n_0}, \quad (19)$$

where we used  $\langle \bar{u}u \rangle_0 = \langle \bar{d}d \rangle_0 = \langle \bar{s}s \rangle_0$  and Eqs. (14)–(16). Note that the leading  $b_1$  correction has disappeared in the ratio of the condensates in Eq. (18).



Also, in the symmetric-matter limit  $n_n = n_p$  (implying  $Z = 1$ ) and neglecting  $\mathcal{O}(w)$  terms, corrections from changes in the chiral condensates vanish. This is at the root of the fact that such effects remain relatively small.

The other effect to be taken into account for the axion-nucleon couplings consists in the in-medium correction to the hadronic matrix elements  $g_A$  and  $g_{ud}^0$ , while finite-density corrections to  $\Delta_s$  (whose contribution to  $c_{p,n}$  is already subleading) can be safely neglected. In-medium corrections to  $g_A$  have been computed in the framework of HBChPT, by taking the matrix elements of the space part of the two-body axial-vector currents and working in the so-called independent-particle approximation for the background nucleons [62], obtaining (see also [21, 63])

$$\frac{(g_A)_n}{g_A} = 1 + \frac{n}{f_\pi^2 \Lambda_\chi} \quad (20)$$

$$\times \left[ \frac{c_D}{4g_A} - \frac{I(m_\pi/k_F)}{3} \left( 2\hat{c}_4 - \hat{c}_3 + \frac{\Lambda_\chi}{2m_N} \right) \right],$$

where  $(g_A)_n$  denotes the hadronic matrix element at finite density,  $\Lambda_\chi \simeq 700$  MeV is the cut-off scale of the chiral Lagrangian,  $k_F = (3\pi^2 n/2)^{1/3} \simeq (270 \text{ MeV})(n/n_0)^{1/3}$  is the Fermi momentum,

$$I(x) = 1 - 3x^2 + 3x^3 \arctan\left(\frac{1}{x}\right), \quad (21)$$

and the low-energy constants (LECs) of the HBChPT Lagrangian are taken to be [63]

$$c_D = -0.85 \pm 2.15, \quad (2\hat{c}_4 - \hat{c}_3) = 9.1 \pm 1.4. \quad (22)$$

Using these values, in Ref. [21] it was estimated

$$\frac{(g_A)_n}{g_A} \simeq 1 - (0.3 \pm 0.2) \frac{n}{n_0}, \quad (23)$$

which, however, is valid only for  $n/n_0 \ll 1$ . Hence, in our numerical analysis we will stick to the more general expression in Eq. (20).

An alternative derivation of the finite density corrections to  $g_A$  was obtained in Ref. [64], based on QCD finite energy sum rules. This result suggests a weaker dependence of  $(g_A)_n$  on the density. The comparison between the abovementioned determinations of  $(g_A)_n$  is displayed in Fig. 2. In the following, we will use the discrepancy between these two results as a further estimate of the theoretical uncertainty.

In principle, one could follow a similar procedure as in Eq. (20) to compute finite density corrections to the iso-singlet matrix element  $g_{ud}^0$ . However, due to the lack of knowledge of the associated LECs, we parametrize the finite density correction as

$$\frac{(g_{ud}^0)_n}{g_{ud}^0} \simeq 1 + \kappa \frac{n}{n_0}, \quad (24)$$

with  $\kappa \in [-0.3, 0.3]$  [21], in analogy to the finite density correction to  $g_A$ .

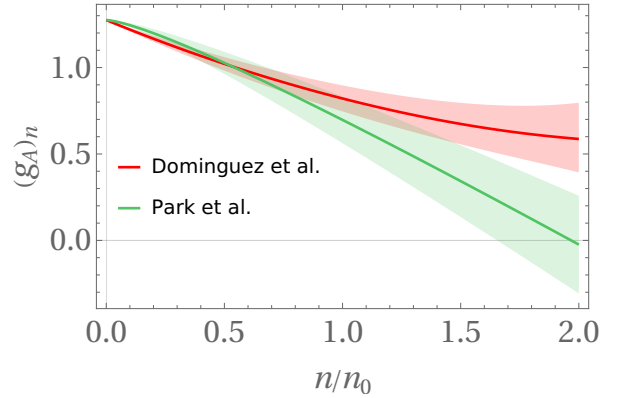


FIG. 2. Comparison between two different determinations of the finite density corrections to  $g_A$ , respectively from Park *et al.* [62] and Dominguez *et al.* [64].

A final comment on meson condensation is in order. At sufficiently high densities, it is expected that a meson condensation phase may occur, leading to significant alterations in hadronic properties (see e.g. Ref. [65]). On the other hand, for symmetric nuclear matter,  $n_p = n/2$ , such effects are expected to arise for  $n/n_0 \gtrsim 2$  [21],<sup>1</sup> that is beyond the regime of validity of the linear approximation in Eqs. (14)–(16). For the SN model considered in this paper (cf. Fig. 1), at  $r \sim 8.5$  km, where the core temperature peaks and axion emission is maximized,  $n/n_0 \sim 1$ . Hence, in the following, we will assume that meson condensation does not occur, which is justified for SN models with  $n/n_0 \lesssim 2$ .

## B. Nucleophobic conditions at finite density

We can now proceed to assess the impact of finite density corrections on nucleophobic axion models. Following the prescriptions described in Sect. IV A, the axion-nucleon coupling combinations in Eqs. (5)–(6) are modified as follows<sup>2</sup>

$$(c_p)_n + (c_n)_n \simeq (c_u^0 + c_d^0 - 1) (g_0^{ud})_n + 2(c_s^0 + r_s^t c_t^0) \Delta_s, \quad (25)$$

$$(c_p)_n - (c_n)_n \simeq (c_u^0 - c_d^0 + (r_u^t - r_d^t) c_t^0 - \frac{1 - zZ}{1 + zZ}) (g_A)_n. \quad (26)$$

The crucial point to be observed is that the nucleophobic conditions in vacuum (cf. Eqs. (7)–(8)) are to a good approximation not affected by finite density corrections. This is due to the multiplicative nature of the corrections due to  $(g_A)_n$  and  $(g_0^{ud})_n$  in Eqs. (25)–(26), as well as to the small effect arising from the  $Z$  correction that is proportional to the

<sup>1</sup> For a related discussion of meson condensation in the SN environment, see also [66, 67].

<sup>2</sup> In this analytical argument we neglect  $\mathcal{O}(w)$  corrections, which are however taken into account in our numerical analysis.

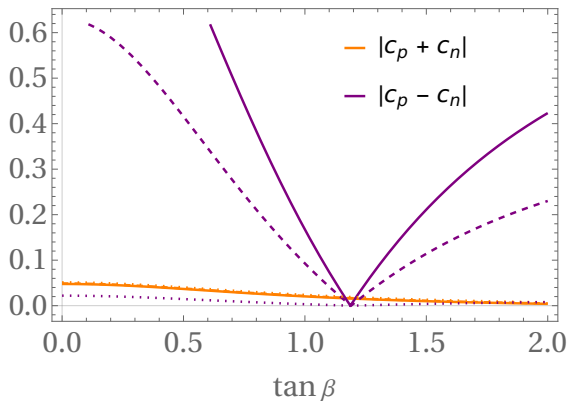


FIG. 3.  $|c_p + c_n|$  (orange) and  $|c_p - c_n|$  (purple, with  $(g_A)_n$  from Ref. [62]) in the M1 model as a function of  $\tan \beta$  and for  $\kappa = 0.3$ , for three values of the density,  $n/n_0 = 0$  (solid lines),  $n/n_0 = 1$  (dashed lines), and  $n/n_0 = 2$  (dotted lines).

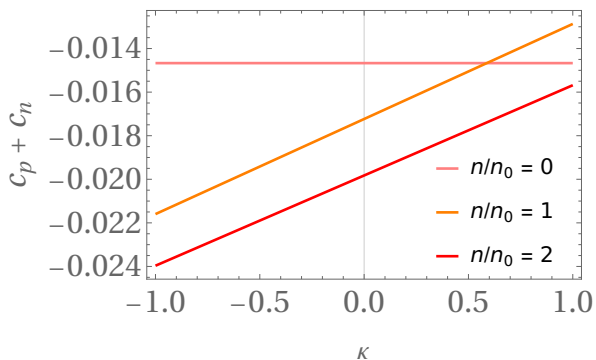


FIG. 4.  $c_p + c_n$  in the M1 model as a function of  $\kappa$ , for  $n/n_0 = 0$  (pink),  $n/n_0 = 1$  (orange),  $n/n_0 = 2$  (red), and for values of  $\tan \beta$  corresponding for each density to the cancellation point  $c_p - c_n = 0$ .

iso-spin breaking  $b_2$  coefficient and to the size of the asymmetry  $(n_n - n_p)/n_0 \lesssim 1$  (cf. Eq. (18)).

Our conclusions are confirmed by the numerical values of the couplings as a function of  $\tan \beta$ , shown in Fig. 3. Remarkably, *i*) density effects lead to a tiny change in the cancellation point for  $|c_p - c_n|$  (not appreciable in Fig. 3), in agreement with our analytical argument; *ii*) the lack of a precise knowledge of the factor  $\kappa$  in the expression for  $(g_{ud}^0)_n$  (cf. Eq. (24)) does not affect the nucleophobic solution at the level of the approximations employed in Eq. (25). Yet, a mild  $\kappa$  dependence is reintroduced via  $\mathcal{O}(w)$  effects, when keeping the full formula in Eq. (5). This can be appreciated from Fig. 4, where we have plotted  $c_p + c_n$  for different values of  $n/n_0$  and for  $\kappa$  varying in the wide range  $[-1, 1]$ . Even taking the worse case scenario of  $\kappa = -1$ , we find  $c_p + c_n \sim -0.022$  for  $n/n_0 = 1$ , which still yields a suppression by a factor of 20 compared to the KSVZ benchmark,  $c_p + c_n \sim -0.43$ . On the other hand, for relatively large positive values of  $\kappa$  the nucleophobic condition can even improve compared to the zero density case.

Finally, Fig. 5 shows the evolution of the values of

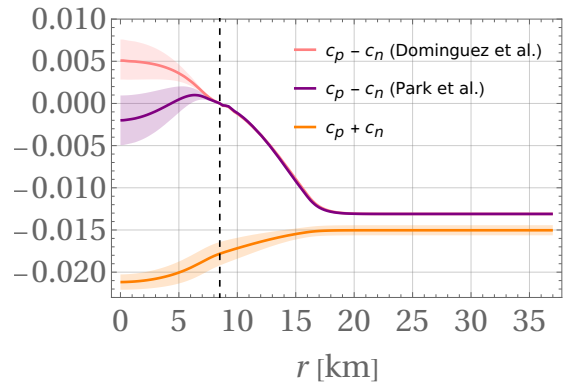


FIG. 5. Density dependence of  $c_p + c_n$  (orange) and  $c_p - c_n$  (purple/red) for the M1 model with  $\kappa = 0$ , and  $\tan \beta$  fixed to the cancellation point of  $c_p - c_n$  at  $r \simeq 8.5$  km (vertical line). The purple line represents the determination of  $(g_A)_n$  from Park *et al.* [62], while the red line corresponds to the determination by Dominguez *et al.* [64]. See text for a description of the parametric uncertainties.

the coupling combinations  $c_p + c_n$  and  $c_p - c_n$  in the M1 axion model as a function of the star's radius  $r$ ,

for the SN density profile depicted in Fig. 1. The variation is due to the change in density and composition of nuclear matter. The parametric uncertainty on  $c_p - c_n$  stems dominantly from the LECs in Eq. (22) (for the case of  $(g_A)_n$  taken from [62]) and the condensates (for the case of  $(g_A)_n$  taken from [64]), whereas the uncertainty on  $c_p + c_n$  is obtained by including the error on  $g_{ud}^0$  and by varying  $\kappa \in [-0.3, 0.3]$ . The value of  $\tan \beta$  has been fixed to enforce the cancellation  $c_p - c_n = 0$  at  $r \simeq 8.5$  km, that corresponds to the shell with the highest temperature, and hence of maximal axion production. Note, however, that due to the dependence of the axion-nucleon coupling on the density, this condition can only be applied locally within a thin shell of the SN core.

## V. REVISING THE SN AXION EMISSION FOR NUCLEOPHOBIC AXIONS

We have shown that the nucleophobia condition can be maintained at high densities and represents a robust feature against density corrections. However, since the SN core does not have a constant density and the axion-nucleon couplings depend on the local environment, nucleophobia cannot be realised uniformly across the entire core. Instead, it can only be enforced within a thin shell where the density and the  $n - p$  asymmetry remains approximately constant. We refer to this scenario as *localized nucleophobia*. Given these premises, a key question from a phenomenological perspective is whether the localized nucleophobia condition is sufficient to relax significantly the SN axion bound.

To quantify this, we compare the energy loss due to axions in our nucleophobic model — where nucle-

ophobia is applied in the shell with maximal temperature — against the same nucleophobic model with couplings independent of density. We perform our numerical analysis using the GARCHING group’s SN model discussed in Sec. III and plotted in Fig. 1. For this estimate, we made a set of simplifying assumptions. First, we neglected the partial degeneracy of nucleons, as most axion emission occurs in the highest temperature regions, where nucleons can be treated as non-degenerate. Second, we focussed on bremsstrahlung production, excluding potential contributions from pion processes [15, 68], as their exact impact on the SN axion emission rate is still uncertain and, in any case, we do not expect them to significantly affect our results. We have also disregarded the corrections to the bremsstrahlung rate that have been recently discussed in the literature (see Ref. [14]), as well as the contribution to the axion emission from strange matter [69].

Since our primary objective is to compare the axion luminosity in two distinct cases using the same set of assumptions, these approximations are not expected to affect significantly our results, and we are confident that our main conclusions remain robust. Lastly, we have performed an integration by summing up the contributions of  $c_n$  over neutron density and of  $c_p$  over proton density, provided by our numerical models (cf. Fig. 1). We ignored interference terms of the form  $c_n c_p$ , which add unnecessary complexity and are somewhat suppressed in their contribution to the emission rate [70].

Using these approximations, the energy emitted in axions per unit time can be calculated through the volume integral [71–73]:

$$L_a(t) \propto \int_0^R \bar{c}_N^2(r) \rho^2(r) T^{7/2}(r) r^2 dr, \quad (27)$$

where  $\bar{c}_N^2 = (c_n X_n)^2 + (c_p X_p)^2$  is an effective axion-nucleon coupling which takes into account the different densities of protons and neutrons, and  $R$  is the star’s radius. Notice that all quantities under integration in the previous equation depend on time, and that constant factors have been omitted as they cancel out when comparing luminosities between axion models.

In Fig. 6 we plot the results of the integration of the luminosity Eq. (27) over the interval  $\Delta t = [1 - 4]$  s post bounce, during which the axion emission is maximal.<sup>3</sup> The figure depicts the SN axion integrated luminosity  $(E_{\Delta t}^{\text{M1}})_n$  for the nucleophobic M1 model, normalized to the luminosity  $(E_{\Delta t}^{\text{M1}})_0$  for the same model without finite density corrections, as a function of the parameter  $\kappa$ . In evaluating  $(E_{\Delta t}^{\text{M1}})_0$ ,  $\tan \beta$  has been fixed to the value that optimizes nucleophobia in vacuum, while for  $(E_{\Delta t}^{\text{M1}})_n$  to the value that optimizes nucleophobia in the shell

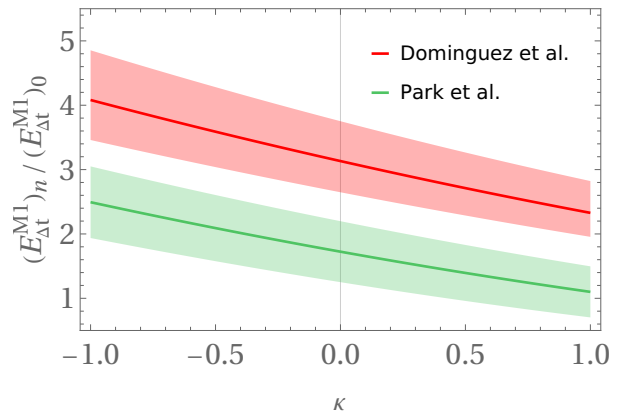


FIG. 6. SN axion luminosity integrated between  $t = 1$  s and 4 s for the nucleophobic M1 model as a function of  $\kappa$ , normalized to the zero density result. The value of  $\tan \beta$  is chosen to optimize nucleophobia respectively in the shell with maximum temperature at  $t = 1$  s, and in vacuum. The two lines correspond to the calculation of  $(g_A)_n$  in Park *et al.* [62] and Dominguez *et al.* [64].

with maximal temperature at  $t \simeq 1$  s. To quantify the theoretical uncertainty, we display two different cases for  $(g_A)_n$ , corresponding to the calculation in Dominguez *et al.* [64] (red line) and in Park *et al.* [62] (green line), where the green band depicts the parametric uncertainty from the LECs in Eq. (22). The difference between the Park *et al.* and Dominguez *et al.* results, shown in the figure, is a consequence of the different behavior of  $g_A$  at high density predicted by the two models, as shown in Fig. 2. This becomes particularly important at late times,  $t \gtrsim 1$  s, when the region of maximal axion production (higher  $T$ ) moves toward the central regions, where the density is higher.

As is evident from the figure, finite density effects tend to reduce the overall level of nucleophobia, since the luminosity is slightly increased. This is not surprising, since in the realistic case, where only the localized nucleophobic condition can be imposed, nucleophobia is less effective than in the vacuum case, where it is possible to impose the nucleophobic condition globally. Nevertheless, the axion time-integrated luminosity calculated with the full density corrections and a realistic SN density profile is only about a factor of 2-4 larger compared to the value obtained when finite density effects are neglected (and even less for certain values of  $\kappa$ ). This corresponds to a bound on the axion mass that is a few times stronger compared to the result  $m_a \lesssim 0.20$  eV obtained in Ref. [13]. The dependence of our result on  $\kappa$  and, in particular, the fact that the ratio between the luminosity in the two cases is suppressed at large  $\kappa$ , stems from the effects of this parameter on the corrections to the axion couplings. In fact, as discussed in Sec. IV, large values of  $\kappa$  may actually reduce the absolute value of the couplings (cf. Fig. 4).

<sup>3</sup> For  $t \lesssim 1$  s relatively low values of the core temperature suppress the emissivity (see e.g. fig. 7 in Ref. [74] or Fig. 11 in Ref. [75]). For  $t \gtrsim 4$  s the temperature quickly drops suppressing again the emissivity.

## VI. CONCLUSIONS

Axion nucleophobia was first proposed in Ref. [13] to address the stringent SN 1987A constraints on QCD axions, which significantly restrict the parameter space relevant to current and future axion search experiments (see, e.g., Refs. [45, 76–79]). These constraints stem from the axion-nucleon couplings. By suppressing this interaction, nucleophobic models [13] allow to expand significantly the viable parameter space, opening up opportunities for new experimental searches.

In this study, we examined the impact of finite density effects on nucleophobic axion models, focusing on the high-density SN core environment. We demonstrated that the nucleophobic condition, which suppresses axion couplings to nucleons, is maintained under in-medium corrections up to supersaturation densities. Additionally, we showed that after the inclusion of finite density effects, nucleophobic axion models still enable a significant relaxation of the stringent SN 1987A axion bound. In particular, with respect to the original (zero density) estimate in Ref. [13], the bound on the axion mass gets strengthened by only a factor between 2 and 4, depending on the specific model assumed for  $g_A$  (cf. Fig. 2). Although the relaxation of the axion bound is less significant compared to the vacuum case (or to the case in which the density and composition of nuclear matter is held constant at certain values) this is a notable result since, as discussed in the text, nucleophobia cannot be imposed throughout the entire SN core and at all times, due to its non-uniform density and composition as well as to the time variations during proto-neutron star core evolution. In other words, the softening of the nucleophobic condition due to the integration over the non-homogeneous SN environment, and over the time interval most relevant for axion emissivity, only partially hinders the relaxation of the SN axion bound. Therefore, nucleophobic axions continue to be a viable possibility for loosening the SN ax-

ion bound, and remain compelling targets for future axion searches.

## ACKNOWLEDGMENTS

We warmly thank Thomas Janka for giving us access to the GARCHING group archive. We also thank Stefan Stelzl for useful communications, and Cristian Villavicencio for clarifications about Ref. [64]. The work of LDL and FM is supported by the European Union – Next Generation EU and by the Italian Ministry of University and Research (MUR) via the PRIN 2022 project n. 2022K4B58X – AxionOrigins. FM and EN are supported in part by the INFN “Iniziativa Specifica” Theoretical Astroparticle Physics (TAsP). The work of EN is also supported by the Estonian Research Council grant PRG1884. EN also acknowledges partial support from the CoE grant TK202 “Foundations of the Universe” and from the CERN and ESA Science Consortium of Estonia, grants RVTT3 and RVTT7. MG acknowledges support from the Spanish Agencia Estatal de Investigación under grant PID2019-108122GB-C31, funded by MCIN/AEI/10.13039/501100011033, and from the “European Union NextGenerationEU/PRTR” (Planes complementarios, Programa de Astrofísica y Física de Altas Energías). He also acknowledges support from grant PGC2022-126078NB-C21, “Aún más allá de los modelos estándar,” funded by MCIN/AEI/10.13039/501100011033 and “ERDF A way of making Europe.” Additionally, MG acknowledges funding from the European Union’s Horizon 2020 research and innovation programme under the European Research Council (ERC) grant agreement ERC-2017-AdG788781 (IAXO+). This article/publication is based upon work from COST Action COSMIC WISPerS CA21106, supported by COST (European Cooperation in Science and Technology).

- 
- [1] R. D. Peccei and H. R. Quinn, *Phys. Rev. Lett.* **38**, 1440 (1977).
  - [2] R. D. Peccei and H. R. Quinn, *Phys. Rev. D* **16**, 1791 (1977).
  - [3] S. Weinberg, *Phys. Rev. Lett.* **40**, 223 (1978).
  - [4] F. Wilczek, *Phys. Rev. Lett.* **40**, 279 (1978).
  - [5] M. Dine and W. Fischler, *Phys. Lett. B* **120**, 137 (1983).
  - [6] L. F. Abbott and P. Sikivie, *Phys. Lett. B* **120**, 133 (1983).
  - [7] J. Preskill, M. B. Wise, and F. Wilczek, *Phys. Lett. B* **120**, 127 (1983).
  - [8] L. Di Luzio, M. Giannotti, E. Nardi, and L. Visinelli, *Phys. Rept.* **870**, 1 (2020), [arXiv:2003.01100 \[hep-ph\]](https://arxiv.org/abs/2003.01100).
  - [9] J. E. Kim, *Phys. Rev. Lett.* **43**, 103 (1979).
  - [10] M. A. Shifman, A. I. Vainshtein, and V. I. Zakharov, *Nucl. Phys. B* **166**, 493 (1980).
  - [11] A. R. Zhitnitsky, *Sov. J. Nucl. Phys.* **31**, 260 (1980), [*Yad. Fiz.*31,497(1980)].
  - [12] M. Dine, W. Fischler, and M. Srednicki, *Phys. Lett. B* **104**, 199 (1981).
  - [13] L. Di Luzio, F. Mescia, E. Nardi, P. Panci, and R. Ziegler, *Phys. Rev. Lett.* **120**, 261803 (2018), [arXiv:1712.04940 \[hep-ph\]](https://arxiv.org/abs/1712.04940).
  - [14] P. Carena, T. Fischer, M. Giannotti, G. Guo, G. Martínez-Pinedo, and A. Mirizzi, *JCAP* **10**, 016 (2019), [Erratum: *JCAP* 05, E01 (2020)], [arXiv:1906.11844 \[hep-ph\]](https://arxiv.org/abs/1906.11844).
  - [15] P. Carena, B. Fore, M. Giannotti, A. Mirizzi, and S. Reddy, *Phys. Rev. Lett.* **126**, 071102 (2021), [arXiv:2010.02943 \[hep-ph\]](https://arxiv.org/abs/2010.02943).



- [16] F. Capozzi and G. Raffelt, *Phys. Rev. D* **102**, 083007 (2020), arXiv:2007.03694 [astro-ph.SR].
- [17] O. Straniero, C. Pallanca, E. Dalessandro, I. Dominguez, F. R. Ferraro, M. Giannotti, A. Mirizzi, and L. Piersanti, *Astron. Astrophys.* **644**, A166 (2020), arXiv:2010.03833 [astro-ph.SR].
- [18] M. M. Miller Bertolami, B. E. Melendez, L. G. Althaus, and J. Isern, *JCAP* **10**, 069 (2014), arXiv:1406.7712 [hep-ph].
- [19] A. H. Córscico, L. G. Althaus, M. M. Miller Bertolami, and S. O. Kepler, *Astron. Astrophys. Rev.* **27**, 7 (2019), arXiv:1907.00115 [astro-ph.SR].
- [20] L. Di Luzio, F. Mescia, E. Nardi, and S. Okawa, *Phys. Rev. D* **106**, 055016 (2022), arXiv:2205.15326 [hep-ph].
- [21] R. Balkin, J. Serra, K. Springmann, and A. Weiler, *JHEP* **07**, 221 (2020), arXiv:2003.04903 [hep-ph].
- [22] S. Stelzl, *How New Particles Change Stars and how Stars Change Particles*, Ph.D. thesis, Munich, Tech. U., Munich, Tech. U. (2022).
- [23] K. Springmann, *How Light Scalars Change the Stellar Landscape*, Ph.D. thesis, Munich, Tech. U. (2023).
- [24] G. Grilli di Cortona, E. Hardy, J. Pardo Vega, and G. Villadoro, *JHEP* **01**, 034 (2016), arXiv:1511.02867 [hep-ph].
- [25] T. Vonk, F.-K. Guo, and U.-G. Meißner, *JHEP* **03**, 138 (2020), arXiv:2001.05327 [hep-ph].
- [26] T. Vonk, F.-K. Guo, and U.-G. Meißner, *JHEP* **08**, 024 (2021), arXiv:2104.10413 [hep-ph].
- [27] K. Choi, S. H. Im, C. B. Park, and S. Yun, *JHEP* **11**, 070 (2017), arXiv:1708.00021 [hep-ph].
- [28] M. Chala, G. Guedes, M. Ramos, and J. Santiago, *Eur. Phys. J. C* **81**, 181 (2021), arXiv:2012.09017 [hep-ph].
- [29] M. Bauer, M. Neubert, S. Renner, M. Schnubel, and A. Thamm, *JHEP* **04**, 063 (2021), arXiv:2012.12272 [hep-ph].
- [30] L. Di Luzio, M. Giannotti, F. Mescia, E. Nardi, S. Okawa, and G. Piazza, *Phys. Rev. D* **108**, 115004 (2023), arXiv:2305.11958 [hep-ph].
- [31] D. Giusti, V. Lubicz, C. Tarantino, G. Martinelli, F. Sanfilippo, S. Simula, and N. Tantalo, *Phys. Rev. D* **95**, 114504 (2017), arXiv:1704.06561 [hep-lat].
- [32] S. Basak *et al.* (MILC), *Phys. Rev. D* **99**, 034503 (2019), arXiv:1807.05556 [hep-lat].
- [33] C. Alexandrou *et al.* (Extended Twisted Mass), *Phys. Rev. D* **104**, 074515 (2021), arXiv:2104.13408 [hep-lat].
- [34] A. Bazavov *et al.*, *Phys. Rev. D* **98**, 074512 (2018), arXiv:1712.09262 [hep-lat].
- [35] A. Bazavov *et al.* (Fermilab Lattice, MILC), *Phys. Rev. D* **90**, 074509 (2014), arXiv:1407.3772 [hep-lat].
- [36] N. Carrasco *et al.* (European Twisted Mass), *Nucl. Phys. B* **887**, 19 (2014), arXiv:1403.4504 [hep-lat].
- [37] S. Navas *et al.* (Particle Data Group), *Phys. Rev. D* **110**, 030001 (2024).
- [38] Flavour Lattice Averaging Group (2024 update) <http://flag.unibe.ch/2021/>.
- [39] Y. Aoki *et al.* (Flavour Lattice Averaging Group (FLAG)), *Eur. Phys. J. C* **82**, 869 (2022), arXiv:2111.09849 [hep-lat].
- [40] J. Liang, Y.-B. Yang, T. Draper, M. Gong, and K.-F. Liu, *Phys. Rev. D* **98**, 074505 (2018), arXiv:1806.08366 [hep-ph].
- [41] K. Choi, S. H. Im, H. J. Kim, and H. Seong, *JHEP* **08**, 058 (2021), arXiv:2106.05816 [hep-ph].
- [42] F. Björkeröth, L. Di Luzio, F. Mescia, and E. Nardi, *JHEP* **02**, 133 (2019), arXiv:1811.09637 [hep-ph].
- [43] F. Björkeröth, L. Di Luzio, F. Mescia, E. Nardi, P. Panci, and R. Ziegler, *Phys. Rev. D* **101**, 035027 (2020), arXiv:1907.06575 [hep-ph].
- [44] M. Badziak, G. Grilli di Cortona, M. Tabet, and R. Ziegler, *JHEP* **10**, 181 (2021), arXiv:2107.09708 [hep-ph].
- [45] L. Di Luzio, M. Fedele, M. Giannotti, F. Mescia, and E. Nardi, *JCAP* **02**, 035 (2022), arXiv:2109.10368 [hep-ph].
- [46] G. Lucente, L. Mastrototaro, P. Carenza, L. Di Luzio, M. Giannotti, and A. Mirizzi, *Phys. Rev. D* **105**, 123020 (2022), arXiv:2203.15812 [hep-ph].
- [47] M. Badziak and K. Harigaya, *JHEP* **06**, 014 (2023), arXiv:2301.09647 [hep-ph].
- [48] F. Takahashi and W. Yin, *Phys. Rev. D* **109**, 035024 (2024), arXiv:2301.10757 [hep-ph].
- [49] M. Badziak, K. Harigaya, M. Łukawski, and R. Ziegler, *JHEP* **09**, 136 (2024), arXiv:2403.05621 [hep-ph].
- [50] “Garching core-collapse supernova research archive,” <https://wwwmpa.mpa-garching.mpg.de/ccsnarchive/>.
- [51] M. Rampp and H. T. Janka, *Astron. Astrophys.* **396**, 361 (2002), arXiv:astro-ph/0203101.
- [52] M. Hempel and J. Schaffner-Bielich, *Nucl. Phys. A* **837**, 210 (2010), arXiv:0911.4073 [nucl-th].
- [53] A. W. Steiner, M. Hempel, and T. Fischer, *Astrophys. J.* **774**, 17 (2013), arXiv:1207.2184 [astro-ph.SR].
- [54] T. Sukhbold, S. Woosley, and A. Heger, *Astrophys. J.* **860**, 93 (2018), arXiv:1710.03243 [astro-ph.HE].
- [55] A. Lella, P. Carenza, G. Co’, G. Lucente, M. Giannotti, A. Mirizzi, and T. Rauscher, *Phys. Rev. D* **109**, 023001 (2024), arXiv:2306.01048 [hep-ph].
- [56] M. Hempel, *Phys. Rev. C* **91**, 055807 (2015), arXiv:1410.6337 [nucl-th].
- [57] T. D. Cohen, R. J. Furnstahl, and D. K. Griegel, *Phys. Rev. C* **45**, 1881 (1992).
- [58] P. Gubler and D. Satow, *Prog. Part. Nucl. Phys.* **106**, 1 (2019), arXiv:1812.00385 [hep-ph].
- [59] U. G. Meißner, J. A. Oller, and A. Wirzba, *Annals Phys.* **297**, 27 (2002), arXiv:nucl-th/0109026.
- [60] N. Kaiser, P. de Homont, and W. Weise, *Phys. Rev. C* **77**, 025204 (2008), arXiv:0711.3154 [nucl-th].
- [61] S. Goda and D. Jido, *Phys. Rev. C* **88**, 065204 (2013), arXiv:1308.2660 [nucl-th].
- [62] T.-S. Park, H. Jung, and D.-P. Min, *Phys. Lett. B* **409**, 26 (1997), arXiv:nucl-th/9704033.
- [63] P. Gysbers *et al.*, *Nature Phys.* **15**, 428 (2019), arXiv:1903.00047 [nucl-th].
- [64] C. A. Dominguez, M. Loewe, C. Villavicencio, and R. Zamora, *Phys. Rev. D* **108**, 074024 (2023), arXiv:2308.05663 [hep-ph].
- [65] M. Mannarelli, *Particles* **2**, 411 (2019), arXiv:1908.02042 [hep-ph].
- [66] J. A. Pons, S. Reddy, P. J. Ellis, M. Prakash, and J. M. Lattimer, *Phys. Rev. C* **62**, 035803 (2000), arXiv:nucl-th/0003008.
- [67] B. Fore and S. Reddy, *Phys. Rev. C* **101**, 035809 (2020), arXiv:1911.02632 [astro-ph.HE].
- [68] T. Fischer, P. Carenza, B. Fore, M. Giannotti, A. Mirizzi, and S. Reddy, *Phys. Rev. D* **104**, 103012

- (2021), arXiv:2108.13726 [hep-ph].
- [69] M. Cavan-Piton, D. Guadagnoli, M. Oertel, H. Seong, and L. Vittorio, *Phys. Rev. Lett.* **133**, 121002 (2024), arXiv:2401.10979 [hep-ph].
- [70] A. Lella, P. Carena, G. Lucente, M. Giannotti, and A. Mirizzi, *Phys. Rev. D* **107**, 103017 (2023), arXiv:2211.13760 [hep-ph].
- [71] G. G. Raffelt, *Stars as laboratories for fundamental physics: The astrophysics of neutrinos, axions, and other weakly interacting particles* (1996).
- [72] M. Giannotti and F. Nesti, *Phys. Rev. D* **72**, 063005 (2005), arXiv:hep-ph/0505090.
- [73] G. Raffelt and D. Seckel, *Phys. Rev. D* **52**, 1780 (1995), arXiv:astro-ph/9312019.
- [74] C. D. Ott, E. Abdikamalov, P. Mösta, R. Haas, S. Drasco, E. P. O'Connor, C. Reisswig, C. A. Meakin, and E. Schnetter, *Astrophys. J.* **768**, 115 (2013), arXiv:1210.6674 [astro-ph.HE].
- [75] K. Sumiyoshi, S. Yamada, H. Suzuki, H. Shen, S. Chiba, and H. Toki, *Astrophys. J.* **629**, 922 (2005), arXiv:astro-ph/0506620.
- [76] I. G. Irastorza and J. Redondo, *Prog. Part. Nucl. Phys.* **102**, 89 (2018), arXiv:1801.08127 [hep-ph].
- [77] P. Sikivie, *Rev. Mod. Phys.* **93**, 015004 (2021), arXiv:2003.02206 [hep-ph].
- [78] E. Armengaud *et al.* (IAXO), *JCAP* **06**, 047 (2019), arXiv:1904.09155 [hep-ph].
- [79] A. Caputo and G. Raffelt, *PoS COSMICWIS-Pers*, 041 (2024), arXiv:2401.13728 [hep-ph].